scientific reports



OPEN

Identification of neutrophil extracellular traps genes as potential biomarkers in psoriasis based on bioinformatics analysis

Yike Zhao 1,2 , Ling Wang 1,2 , Xiaoguang Zhang 1 , Lihua Zhang 1 , Feng Wei 1 , Suyue Li 1 & Yanling Li $^{1 \boxtimes}$

The epidermal infiltration of neutrophils is a hallmark of psoriasis (PSO) and its activation leads to the release of neutrophil extracellular traps (NETs). However, the molecular mechanism of NETsrelated genes (NETRGs) has not been extensively studied in PSO. To define NETs-related-biomarkers for PSO. The GSE13355 and GSE78097 datasets, and NETRGs gene set were included in this study. The datasets used in this study were all microarray data. The weighted gene co-expression network analysis (WGCNA) and machine learning algorithms were used to mine key genes. Later on, singlegene gene set enrichment analysis (GSEA) and immune infiltration analysis were implemented. Finally, the expression of key genes was verified using quantitative real-time fluorescence PCR (qRT-PCR). A total of 3 key genes (S100A9, CLEC7A, and CXCR4) were derived, and they all had excellent diagnostic performance. The single-gene GSEA enrichment results indicated that the key genes were mainly enriched in the chemokine signaling pathway and humoral immune response in the high-expression group, while focal adhesion was enriched in the low-expression group. The correlation analysis indicated that all key genes were strongly negatively correlated with resting mast cells and TGF-β family member receptor, while they were strongly positively correlated with activated CD4 memory T cells and antigen processing and presentation. Lastly, the experimental results showed that the expression trends of key genes were consistent with public database. In this study, we successfully screened three potential PSO diagnostic genes (S100A9, CLEC7A and CXCR4) that were closely related to NETs, and these findings not only provided new molecular marker candidates for the precise diagnosis of PSO patients, but also revealed possible future therapeutic targets. However, further indepth research and validation were necessary.

Keywords Psoriasis, Neutrophil extracellular traps, Diagnosis, Immunity

Psoriasis (PSO) is a chronic autoimmune skin disease characterized by erythema and plaques¹. It is considered that interaction of activated keratinocytes with infiltrated immune cells in the skin is the major driver of PSO pathogenesis¹⁻³. PSO can occur on any part of the body, most commonly affecting trunk, gluteal fold and scalp^{4,5}. PSO can be diagnosed clinically in most patient, while a skin biopsy ought to be required in the patients of atypical presentation. Treatment for patients with mild PSO mainly of topical therapy, such as corticosteroids, Vitamin D analogues, Calcineurin inhibitors, kertolytics and targeted light therapy. For patients with moderated to severe PSO, treatments for PSO do not include phototherapy, but include oral systemic therapy and biologic therapy⁵. In real-world applications of PSO, treatment satisfaction, effectiveness and safety can be increased by adding antimetabolites medication to biologics, but they can not cure disease completely⁶. Therefore, it is necessary to find the new biomarkers to diagnose PSO as soon as possible.

Neutrophils as the first line of defense in innate immunity, which are the most abundant immune cells in humans^{7,8}. Neutrophils can contribute to various tissue repair, but exaggerated neutrophils activation are linked to immunopathology of various diseases^{8,9}. Neutrophils may undergo a process of cell death after activation, which called NETosis. It is called as neutrophil extracellular traps (NETs), where intra-nuclear material is

¹Department of Dermatology, Clinical Medical Research Center of Dermatology and Venereology in Hebei Province, Construction Unit of the Sub-Center of the National Center for Clinical Medical Research On Skin and Immunological Diseases, The Second Hospital of Hebei Medical University, Shijiazhuang, Hebei, People's Republic of China. ²These authors contributed equally: Yike Zhao and Ling Wang. [™]email: doctorlyl@hb2h.com

extruded to extracellular. NETs are considered as DNA structures¹⁰. The structure of NETs contain decondensed DNA, granular proteins and histones, released from neutrophils by stimulation¹¹. NETs could entrap microorganisms¹⁰. A large amount of inflammatory mediators are exposed and media ted the inflammatory responses in the formation of NETs¹. The NETs contribute to autoinflammatory diseases, and it can be initiated by stimulation, such as immune complexes, autoantibodies¹⁴. Some recent studies have indicated that patients with PSO exhibit a unique circulation of leukocytes and the increased neutrophil counts in many studies¹². Recent studies have demonstrated that NETs exist in PSO skin and induces the production of inflammatory cytokines¹. And it also can promote Th17 cell differentiation, driving the immune disorder in PSO patients¹³. However, the role of NETs in pathogenesis of PSO is still unclear enough.

This study was carried out based on PSO transcriptome data in the public database. Three key genes related with NETs were screened and its diagnosis values were explored by a series of bioinformatics tools such as analyzing differentially expressed genes and weighted correlation network analysis (WGCNA). Moreover, we also explored the related pathways and molecular mechanisms, which provided the basis for investigating the molecular mechanisms based on NETs and PSO.

Materials and methods Source of data

The GSE13355 and GSE78097 datasets were sourced from the GEO database. The GSE13355 dataset, including 58 PSO samples and 64 control samples, was utilized as a training cohort. The GSE78097 dataset, includin 27 PSO samples and 6 control samples, was utilized as a validation cohort. The datasets used in this study were all microarray data, and the sample types were all tissue samples. Then, 136 neutrophil extracellular traps-related genes (NETRGs) (Supplementary Table 1) were obtained from previous report¹⁴.

Identification of DEGs

Differential expressed genes (DEGs) between the PSO and control groups were selected by the limma package (v 3.48.3) with adjusted P value < 0.05 and $|\log_2 FC| > 1^{15}$. The results were illustrated by the ggplot2 package (v 3.3.5) and pheatmap package (v 1.0.12) respectively¹⁶. Then, the Uniform Manifold Approximation and Projection (UMAP) was performed on all samples based on the DEGs.

Filtering for key module genes by WGCNA

The co-expression network was constructed by WGCNA (v 1.70–3) in the training cohort 17 . Firstly, the samples were clustered and outliers were removed to ensure the accuracy of the analysis. Then, the optimal soft threshold (β) were chosen to make the network approximated a scale-free distribution. In the following, the cluster dendrogram was gained via calculating adjacency and similarity. The modules were partitioned by dynamic tree cutting algorithm. The MEDissThres was then set to 0.5 to merge similar modules. Next, we evaluated the correlation between each module and PSO, and selected the module with the highest absolute value of correlation coefficient with PSO as the key module. Finally, the genes in the key module with |GS| > 0.5, P value ≤ 0.05 , and |MM| > 0.5 were identified as key module genes for follow-up analysis.

Screening and functional enrichment of candidate genes

The candidate genes were filtered by overlapping key module genes, DEGs, and NETRGs. Then, chromosomal localization analysis of candidate genes was performed by the RCircos package (v 1.2.2). A PPI network was created on the basis of candidate genes via the STRING database. Gene Ontology (GO) and Kyoto Encyclopedia of Genes and Genomes (KEGG) enrichment analyses of candidate genes were implemented via clusterProfiler package (v 4.0.2) 18 . A significant enrichment analysis result was defined with adjusted P value < 0.05 and a count value ≥ 1 .

Machine learning screening and performance evaluation of key genes

Two machine learning models were constructed based on candidate genes to screen key genes separately. LASSO regression profiling was carried out using the glmnet package (v 4.1–4) to obtain LASSO-feature genes¹⁹. Next, SVM analysis was performed, and the recursive feature elimination (RFE) method was used to obtain the importance ranking of each genes and the rate of error for each iteration of the combination. Finally, the genes included in the portfolio with the lowest error rate were selected as SVM-RFE-feature genes. The key genes were screened by overlapping LASSO-feature genes and SVM-RFE-feature genes. To explore the ability of key genes to distinguish between control and PSO groups, ROC curves were plotted. Then, the AUC values of ROC curve were computed using the pROC package (v 1.18.0)²⁰. Finally, the expression levels of key genes between control and PSO groups were compared in the training and the validation cohorts, respectively.

Construction of the nomogram

In this study, the nomogram was structured and visualized on the basis of key genes by rms package (v 6.1–0). Next, calibration curve was plotted to judge the model prediction performance.

Single-gene GSEA analysis

The samples were classified into high- and low-expression groups using the median value of key genes expression. Then, single-gene GSEA was performed to find the enriched regulatory pathways and biological functions between the high- and low-expression groups via clusterProfiler (v 4.0.2) and org.Hs.eg.db (v 3.13.0) package with |NES| > 1, q < 0.25, and NOM P value $< 0.05^{18}$. The top 10 results for GO and KEGG significance were visualized separately.

Immuno-infiltration analysis

The proportion of 22 immune cell subtypes were computed for each samples by the CIBERSORT algorithm in the training cohort²¹. Afterwards, the differential immune cells between PSO and control groups were compared and box-plot was plotted. Meanwhile, the correlation analysis was performed between immune cells and key genes. In addition, the difference in each immune response score between the PSO and control groups was computed using the GSVA package and the results were presented by box plot. The immune response geneset was obtained from the ImmPort database²². Finally, the correlation between key genes and differential immune responses was analyzed by the Spearman method.

Construction of ceRNA network

The miRWalk database was used to predict miRNAs targeting key genes. Meanwhile, the miRDB database was utilized for targeting miRNA prediction for key genes. The common miRNAs (co-miRNAs) were obtained by taking the intersection of the predicted miRNAs from the two databases. Next, the miRTarBase database was utilized to predict target lncRNAs targeting the co-miRNAs. Finally, a sankey diagram of the lncRNA-miRNA-mRNA network was constructed on the basis of these miRNAs and lncRNAs using the Sangerbox.

Construction of key gene-drug interaction network

The drugs targeting the key genes were predicted through the DGIdb database (https://dgidb.org). A key genedrug network was constructed based on the predicted results.

Construction of key gene-disease relationship networks

The diseases associated with key genes were obtained using the DisGeNET database and a network of key genedisease relationships was constructed (Score gda > 0.1).

RNA isolation and quantitative real-time polymerase chain reaction (qRT-PCR)

Ethical approval for this study was obtained from the ethics committee of the second hospital of Hebei Medical University (2023-R331). Tissues of PSO samples were diagnosed as PSO by biopsy. Tissues of control samples were all from healthy samples. Twenty tissues (10 PSO samples, and 10 control samples) were lysed with TRIzol reagent and total RNA was isolated following the manufacturer's instructions. The concentration of RNA was measured with a NanoPhotometer N50. Then, RNA was reverse transcribed into cDNA using the SureScript First strand cDNA synthesis kit (Servicebio, Wuhan, China). The qRT-PCR reaction consisted of 3 μ L of reverse transcription product, 5 μ L of 2xUniversal Blue SYBR Green qPCR Master Mix, and 1 μ L each of forward and reverse primer. All primer sequence information were shown in Supplementary Table 2. The GAPDH gene served as an internal control, and the relative expression of genes was determined using the $2^{-\Delta\Delta CT}$ method²³. Graphpad Prism 5 was used to make the graph and calculate the p-value.

Ethical approval

This study was performed in line with the principles of the Declaration of Helskinki. Ethical approval for this study was obtained from the ethics committee of the second hospital of Hebei Medical University (2023-R331). Informed consent was obtained from all subjects and/or their legal guardians.

Statistical analysis

All bioinformatics analyses were carried out in R language. Spearman correlation analysis was used to conduct the correlation analysis.

Results

Identification of DEGs and immune infiltration analysis

In total, 597 DEGs between the PSO and control groups were gained, including 407 up-regulated genes and 190 down-regulated genes (Fig. 1A,B, Supplementary Table 3). Immediately after, the results of UMAP indicated that the DEGs were able to distinguish the two groups of samples excellently (Fig. 1C).

Identification of key module genes

To probe for genes associated with PSO, we performed WGCNA analysis. Sample clustering results showed there were no outlier samples (Fig. 2A). With a soft threshold equal to 5, $R^2 = 0.85$ (red line), and average connectivity close to 0, the interactions between genes maximally conform to a scale-free distribution (Fig. 2B). A total of 12 modules were obtained by the dynamic tree cut algorithm (Fig. 2C). After merging similar modules 8 modules were obtained (Fig. 2D). Of these, MEturquoise (Cor = 0.95, P = 2e-61) showed the highest correlation with PSO (Fig. 2E). Therefore this module was considered as key module. Finally, the 5084 genes in this module were defined as key module genes for subsequent analysis (Fig. 2F).

Identification and functional annotation of candidate genes

A total of 14 candidate genes (S100A12, S100A9, CLEC7A, CXCR4, IL36RN, CD274, LTF, MMP9, F3, IRF1, CXCL1, S100A8, CCL2, and LYZ) were filtered by overlapping 136 NETRGs, 5084 key module genes, and 597 DEGs (Fig. 3A). The results of chromosomal localization analysis indicated that the majority of candidate genes were located on autosomes (Fig. 3B). The PPI network had 14 points and 35 edges (CCL2-S100A9, CXCR4-MMP9, LYZ-S100A8 and so on) (Fig. 3C). In addition, the results of the enrichment analysis indicated that the candidate genes implicated 270 GO entries and 6 KEGG pathways²⁴⁻²⁶. The candidate genes were mainly

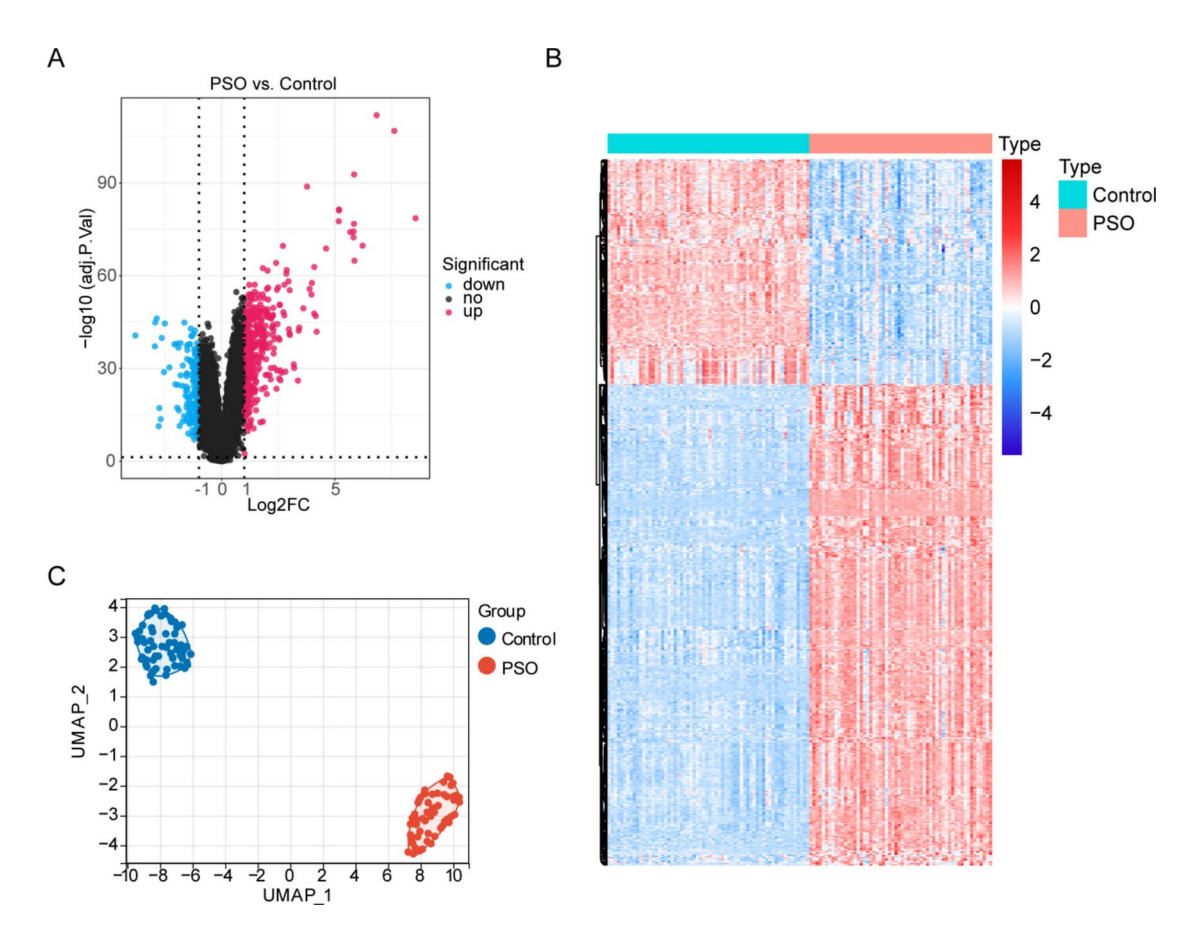


Fig. 1. Differential expression analysis in the GSE13355 dataset. (**A, B**) The volcano map (**A**) and heat map (**B**) of differentially expressed genes (DEGs) between psoriasis (PSO) and control groups. (**C**) The Uniform Manifold Approximation and Projection (UMAP) results of DEGs.

enriched to GO entries such as defense response to fungus, neutrophil chemotaxistc, etc. (Fig. 3D, Supplementary Table 4). KEGG enrichment results included TNF signaling pathway, etc. (Fig. 3E, Supplementary Table 4)^{24,26}.

Identification and expression of key genes

A total of 4 LASSO-feature genes (S100A12, S100A9, CLEC7A, and CXCR4) were screened by LASSO regression analysis (Fig. 4A,B). The error rate and the correct rate were computed and found that the SVM model had the lowest error rate and the highest correct rate when it contained 4 genes (Fig. 4C,D). Therefore, these 4 genes were selected as SVM-RFE-feature genes (S100A9, CXCR4, IL36RN, and CLEC7A) for further analysis. Hence, a total of 3 key genes (S100A9, CLEC7A, and CXCR4) were screened by overlapping LASSO-feature genes and SVM-RFE-feature genes (Fig. 4E).

The results of ROC curves for the training cohort demonstrated the excellent diagnostic performance of the key genes with AUC values equal to 1 (Fig. 5A). The diagnostic effectiveness of key genes was well demonstrated in the validation cohort (Fig. 5B). Then, the expression of key genes in PSO group was significantly higher than that in control group in the training cohort, and the trend of expression in the validation cohort was consistent with it (Fig. 5C,D).

Construction of the nomogram

The nomogram on the basis of 3 key genes was utilized to predict the risk of developing PSO in patients (Fig. 5E). As illustrated by the calibration curve, the precision of the nomogram was excellent (Fig. 5F).

GSEA analysis of two different expression subgroups

The main outcomes of KEGG enrichment in the high-expression group included cell cycle, chemokine signaling pathway, etc. (Supplementary Fig. 1A–C, Supplementary Table 5)^{24–26}. GSEA results indicated that the signature were mainly enriched to KEGG terms in low-expression groups such as focal adhesion, etc. (Supplementary Fig. 1A–C, Supplementary Table 5)^{24,26}. The major results of GO enrichment in the low-expression group consisted of extracellular matrix structural constituent, etc. (Supplementary Fig. 1D–F, Supplementary Table 6). The signature were mainly enriched to GO terms in high-expression groups such as antimicrobial humoral response, humoral immune response, etc. (Supplementary Fig. 1D–F, Supplementary Table 6).

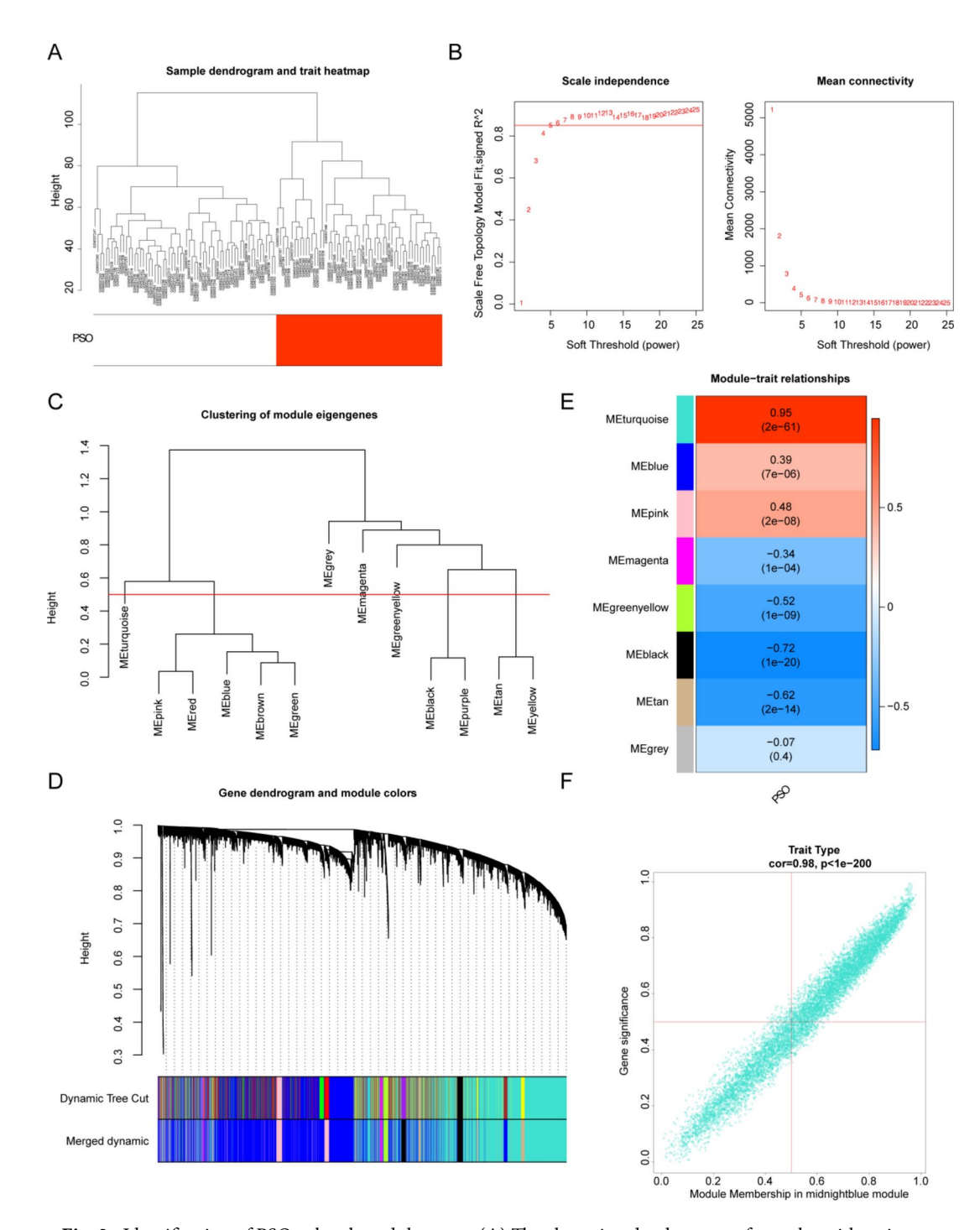


Fig. 2. Identification of PSO-related module genes. (A) The clustering dendrogram of samples with trait heatmap. (B) Selection of the optimal soft-thresholding (power). (C) Clustering of module eigengenes. (D) Hierarchical clustering of genes and module identification. (E) Heatmap of the relationships between gene modules and PSO. (F) The scatter plot of the relationship between module membership (MM) and gene significance (GS) in the midnightblue module.

Immune-related analyses of key genes

The bars showed the proportion of the 22 immune cells in each sample (Fig. 6A). In total, 18 immune cells (CD8 T cells, resting mast cells, resting NK cells, neutrophils, etc.) were significantly different between the PSO and control groups (Fig. 6B). The correlation analysis indicated that all key genes were strongly negatively correlated with resting mast cells, while they were strongly positively correlated with activated CD4 memory T cells (Fig. 6C). There were 15 differential immune responses (interferons, BCR signaling pathway, cytokines, etc.) between the POS and control groups identified by the Wilcoxon test (Fig. 6D). The correlation analysis

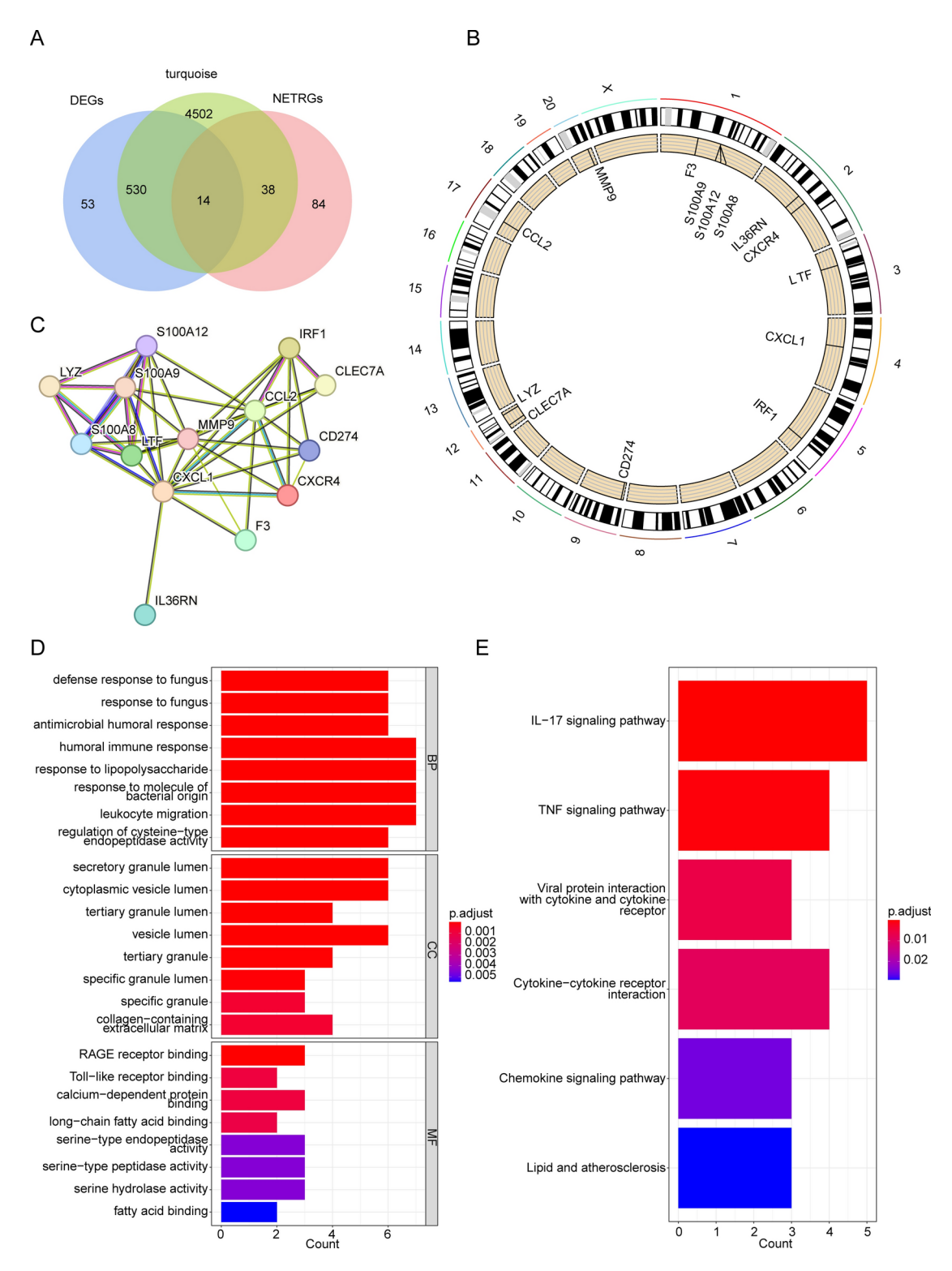


Fig. 3. Identification of candidate key genes and functional enrichment analysis. (**A**) The venn diagram of 14 candidate genes. (**B**) The chromosomal localization results of 14 candidate genes. (**C**) The protein–protein interaction (PPI) network of candidate key genes. (**D**) The Gene Ontology (GO) terms enriched in candidate genes. BP, biological progress (BP); CC, cellular component; MF, molecular function. (**E**) The Kyoto Encyclopedia of Genes and Genomes (KEGG) pathways enriched in candidate genes.

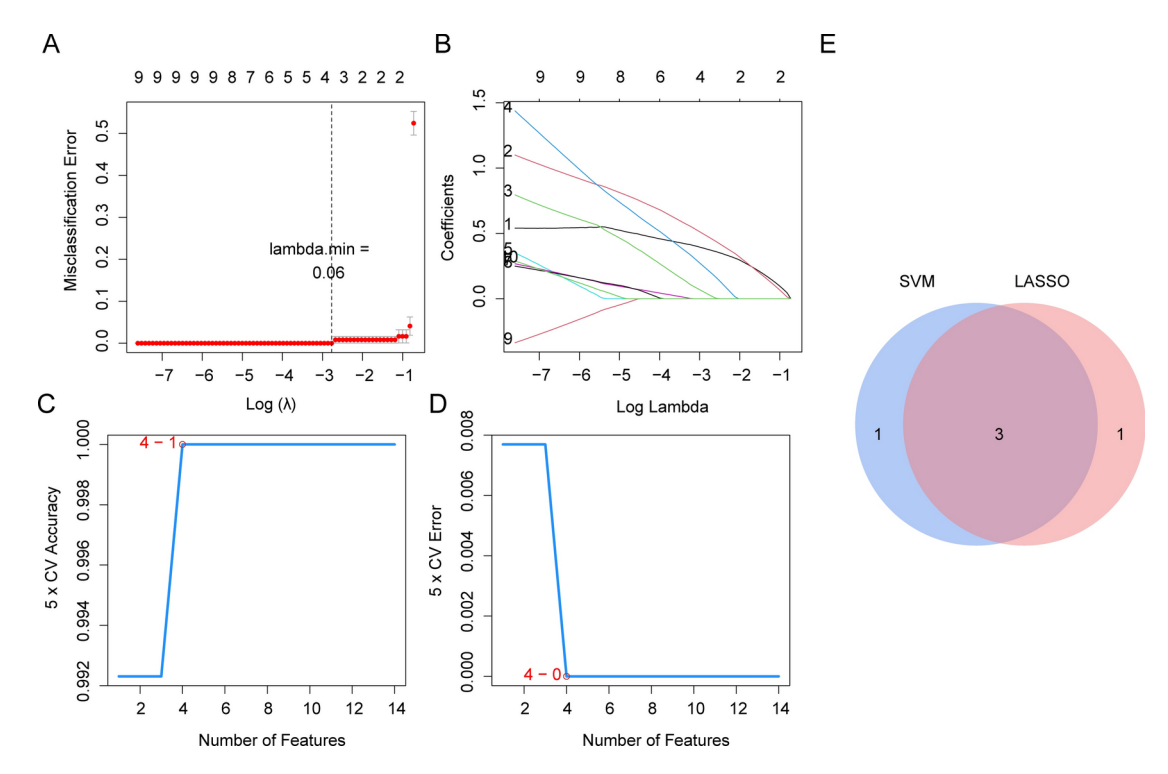


Fig. 4. Identification of key genes by machine learning algorithms. (**A, B**) The error plot for tenfold cross-validation (**B**) and the plot of gene coefficients (**B**) in least absolute shrinkage and selection operator (LASSO) analysis. (**C, D**) The genes filtered by support vector machine recursive feature elimination (SVM-RFE). (**E**) The venn diagram of 3 key genes.

illustrated that key genes had a strong negative correlation with TGF- β family member receptor, which had a strong positive correlation with antigen processing and presentation (Fig. 6E).

The ceRNA regulatory network of key genes

Based on key genes we obtained 5 co-miRNAs (hsa-miR-660-3p, hsa-miR-9-5p, hsa-miR-663b, hsa-miR-613, and hsa-miR-342-3p) and 6 lncRNAs (MALAT1, C17orf102, C1orf147, ELFN2, TMEM105, and SNHG16). The specific mRNA-miRNA pairs were CXCR4-hsa-miR-9-5p, etc., and the lncRNA-miRNA pairs were SNHG16-hsa-let-7b-5p, etc. (Supplementary Fig. 2A).

Prediction of therapeutic agents of key genes

Through DGIdb database, 3 key genes were found that targeted by 30 therapeutic drugs (Supplementary Fig. 2B). The network included 2 drugs (Tasquinimod and Paquinimod) for S100A9, 8 drugs (Ellagic acid, Tamatinib and so on) for CLEC7A, and 20 drugs (Mavorixafor, Chembl2347633, Cisplatin and so on) for CXCR4 (Supplementary Fig. 2B).

Establishment of key gene-disease networks

The network included 55 diseases (WHIM syndrome, Rheumatoid Arthritis, Malignant neoplasm of breast, Neoplasm Metastasis, etc.) and 3 key genes (Supplementary Table 7). Of these, 9 diseases (Malignant tumor of colon, Schizophrenia, Celiac Disease, Colonic Neoplasms, etc.) were related to S100A9, 5 diseases (Aspergillosis, Candidiasis, Chronic Mucocutaneous, Candidiasis, Familial, 2, Hepatitis, and Onychomycosis) were related to CLEC7A and 41 diseases (Neoplasm Metastasis, Breast Carcinoma, Mammary Neoplasms, etc.) were related to CXCR4 (Supplementary Fig. 3A).

Expression validation of 3 key genes

In this study, 10 pairs of PSO and control tissue samples were collected and qRT-PCR was performed to elucidate the changes in expression of key genes in the PSO and control groups. The expression levels of key genes were significantly lower in control samples than in PSO tissues, which was consistent with results from public database (Supplementary Fig. 3B).

Discussion

PSO is a prevalent skin disease, mediated by T cells. T cells, especially neutrophils could trigger NETosis and neutrophil migration²⁷. A large amount of inflammatory mediators could be exposed and an inflammatory responses might be mediated while NETs are forming. And many recent studies have shown that NETs may be exist in PSO lesions ¹. Aberrant gene expression is clearly closely related to many pathological processes

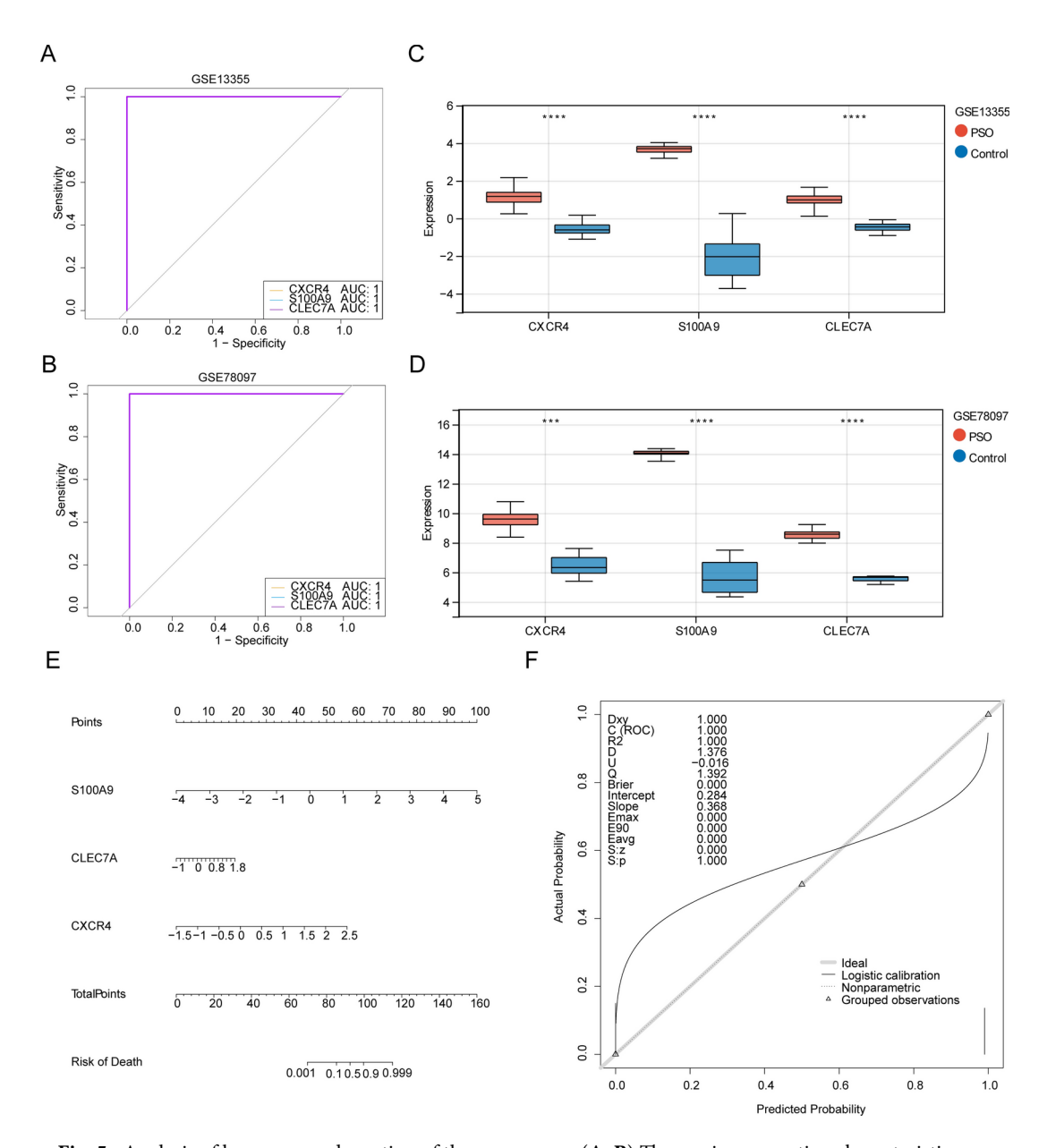


Fig. 5. Analysis of key genes and creation of the nomogram. (**A, B**) The receiver operating characteristic (ROC) curves of key genes in the GSE13355 (**A**) and GSE78097 (**B**) datasets. (**C,D**) The expression levels of key genes between PSO and control groups in the GSE13355 (**C**) and GSE78097 (**D**) datasets. (**E**) The nomogram established based on three key genes. (F) The calibration curve of the nomogram.

in PSO. The absence in melanoma 2 (AIM2) is a susceptibility gene locus for psoriasis has been proven²⁸. The formation of NETs and high expression of the AIM2 gene can be detected in psoriasis. And it might be considered that NETs promote the expression of AIM2 gene by activation of keratinocytes²⁹. In addition, the high expression of FOSL1 gene is the markers of psoriasis ^{29,30}. The transcription factor PPAR-γ is a proportional network that combines multiple transcription factors. The transcription factor PPAR-γ could appear upstream of AP1 and NF-κB. And PPAR-γ can be under the control of FOXO1³¹. Otherwise, IL-23R, IL-23 and FTO, MC4R and LNPEP, AGT, eNOS genes are shared genetic background with psoriasis, atherosclerosis, obesity and hypertension, respectively^{32–38}. Therefore, the NETs-related PSO diagnostic genes were screened using a bioinformatics approach in this study. Meanwhile, this study performed integrated bioinformatic analysis of changes in the expression of crucial genes to reveal potential pathways and gene interactions involved after the development of PSO based on RNA-seq results.

BP annotation revealed that the DEGs of PSO were significantly enriched in the defense response to fungus, response to fungus, antimicrobial humoral response, humoral immune response, response to lipopolysaccharide, response to molecule of bacterial origin, leukocyte migration and regulation of cysteine-type endopeptidase activity, which are all related to immune responses. PSO is a chronic T cell-mediated inflammatory skin disease, with innate immunity playing an essential role³⁹. The genes identified here suggested that immune response

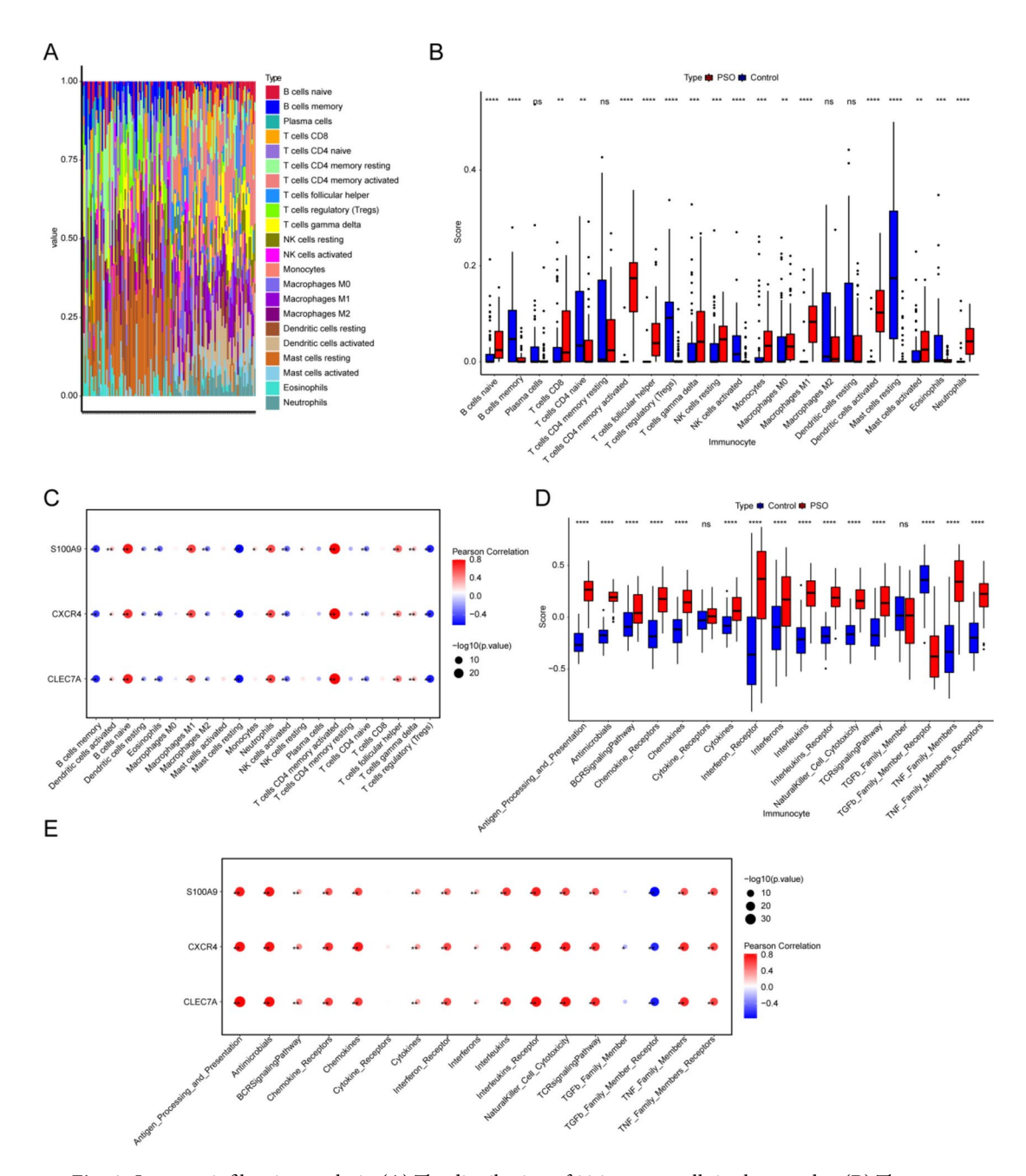


Fig. 6. Immune infiltration analysis. (**A**) The distribution of 22 immune cells in the samples. (**B**) The discrepancies of immune cells between PSO and control samples. ns, not significant; ** p < 0.01; ****p < 0.001; ****p < 0.001. (**C**) The relevance of key genes to differential immune cells. Red circles represent positively correlation and blue circles represent negatively correlation. *p < 0.05; ** p < 0.01. (**D**) Comparison of the scores of immune pathways between PSO and control groups. ns, not significant; ****p < 0.0001. (E) The relevance of key genes to differential immune pathways. Red circles represent positively correlation and blue circles represent negatively correlation. *p < 0.05; ** p < 0.01.

activation acts as an essential trigger in PSO and NETs. KEGG enrichment analysis showed that the IL-17 signaling pathway and TNF signaling pathway were the most important pathways in PSO 24,26 . IL-17 signaling pathway activation would contribute to the coordinate local of tissue inflammation, and activated T cells mainly secreted IL-17 cytokines as the key mediators in PSO 40 . Thus, the IL-17 signaling pathway may strongly correlate with PSO development. Th17 cells can secrete IL-17 and TNF- α , which can induce keratinocyte proliferation, increase the expression of endothelial adhesion molecules and angiogenic mediators, causing the immune cells to infiltrate into PSO skin 5 .

IL-10 are considered as one of the IL-10 gene cluster, the other three genes are IL-19, IL-20 and IL-24, which were formed as IL-19 subfamily. IL-19 subfamily have been indicated the role in the pathogenesis of psoriasis⁴¹. As it is known, IL-19 is proinflammatory cytokine, which may have role in the development of psoriasis, but

also induces TNF- α and IL-6 production and apoptosis in monocytes. Previously, associated with IL-19 and IL-20 genes, CACCGGAA haplotype was related to an increased risk of psoriasis⁴². Working together with IL-19 and IL-36, IL-22 plays an essential role in epidermal hyperplasia and parakeratosis⁴³. IL-22 is required for the pathogenesis and development of psoriasis. And deficiency of IL-22 caused a significant decrease in dermal inflammation induced by IL-23⁴⁴. IL-22 is considered as an essential cytokine for psoriasis, but the clinical trial all failed because of the unreachable expected endpoints ⁴⁴. Latest research found that patients who have the deficiency of autoantibody to both IL-12B/IL-22 or IL-12B/IL-17A tended to have higher PASI score⁴⁵. It suggests that low-level antibody of IL-22 might be associated with the development of psoriasis. These findings point to a critical role of IL-22 in pathogenesis of psoriasis together, suggesting that targeted IL-22 therapeutic agents are expected to be a promising new strategy for the treatment of psoriasis.

In our study, the top three DEGs in the miRNA-gene network were S100A9, CLEC7A, and CXCR4. S100A9 is one of calcium-binding proteins up-regulated in inflammatory conditions 46,47. The S100A9 proteins are related to abnormal keratinocyte differentiation located with the epidermal differentiation complex on chromosome 1q21⁴⁸. In inflammatory condition, the main S100A9 expressing cells are neutrophils, keratinocytes and macrophages^{47,49,50}. S100A9 is expressed in high amounts in monocytes and neutrophils, but not in macrophages, lymphocytes or dendritic cells in mature tissues⁵¹. S100A9 accounting for 40% of cytosolic proteins in neutrophils^{46,52}. The animal studies have shown that S100A9 is associated with PSO-like epidermal and its absence lead to more severe PSO⁴⁶. S100A9 in epidermal modulates neutrophils recruitment to inflammatory sites, and neutrophil-related proteins and pathways in skin are affected by \$100A9 in epidermis⁴⁶. During the skin inflammation, cytokine and chemokine expressions are modulated by epidermal \$100A946. It is reported that S100A9 expression is induced in inflammatory activation of keratinocytes⁵¹. Whereas S100A9 is highly up-regulated in skin lesions of psoriasis patients, it is reported that a significant increase of S100A9 expression in keratinocytes⁵¹. Obvious studies have discovered that Dectin-1 receptor is encoded by the CLEC7A gene, and its decrease could mediate the induction of regulatory dendritic cells (DCs)⁵³. Otherwise, CLEC7A gene is expressed on neutrophils, macrophages and monocytes, and it has been shown to recognize a broad range of fungi and bacteria, causing cancer and autoimmune disorders⁵⁴. It is considered that the CLEC7A gene encodes the Dectin-1 receptor and is highly associated with the production of IL-1 β^{55} . Obvious findings have revealed that the transcripts of CLEC7A is highly correlated with interleukins and chemokines⁵⁶. The Dectin-1 protein forming the cell walls of fungi and pathogenic bacteria, takes efforts to against fungal infections through immune signaling and pathogenic recognition⁵⁷. Therefore, down-regulated of CLEC7A may correlate with the development of PSO. Elevated level of CLEC7A gene transcripts is associated with defective production of IL-10. IL-10 is considered a potent regulatory cytokine with proinflammatory role⁵⁶. Only the psoriatic fibroblasts express CXCL12, which contribute to the recruitment of CXCR4+Tc17 cells⁵⁸. So we can concentrate on the relationship between CXCR4 gene and PSO.

Additionally, some research found that the expression of autophagy-related genes could be considered as potential biomarkers for diagnosis of psoriasis, such as BIRC5, NAMPT and BCL2)⁵⁹. And it has been reported that ATG16L1 gene contributes to the psoriasis⁶⁰. Some autophagy-related genes, like ATG16L1 and BIRC5, have significant diagnostic value in early psoriasis vulgaris. They might influence pathological progress of psoriasis by regulating the process of autophagy^{60,61}. Therefore, we plan to explore the role of autophagy genes like ATG16L1 in psoriasis and their interaction network to fully understand the pathogenesis of psoriasis in future.

To explore possible effective treatments for PSO, we used the DGIdb database to determine therapeutic drugs or molecular compounds that could restore dysregulated expression of DEGs. Almost of the predicted drugs have been used in clinical treatment for PSO, and further studies are urgently needed to evaluate their capacity for clinical application. Previous studies have often focused on a single method or datasets, lacking of comprehensiveness and systematic system. Our study used powerful data-driven approach, like WGCNA and machine learning algorithm. And our study integrated two high-quality datasets of GSE13355 and GSE78097 and identified three biomarkers. But our study has some limitations. Further studies should be done to investigate and verify whether the three biomarkers identified in our study are involved in PSO and explore their potential mechanisms. Besides, given that we only performed transcriptomic analysis of PSO, it would be helpful if other omics analysis, proteomics and metabomomics, could be performed to fully understand the biological mechanism of psoriasis. Given the limited sample size for our current RNA-seq analysis, we recognize that expanding the sequencing scale, such as adding additional RNA-seq datasets, and conducting a large range of studies are essential to further validate and deepen our findings. Finally, whether the discovered biomarkers can distinguish between psoriasis and other skin diseases remains to be further explored. In the future, in order to further validate the specificity and sensitivity of these biomarkers, we could add datasets and conduct comparative analysis with other skin diseases to explore the commonality and differences of biomarkers between different diseases.

In summary, we revealed the PSO-related pathways, predicted possible regulatory mechanisms, and explored promising drugs for PSO. Thus, our study provided potential targets for future research.

Data availability

The gene expression profiles of GSE13355 and GSE78097 were downloaded from Gene Expression Omnibus GEO (https://www.ncbi.nlm.nih.gov/geo/query/acc.cgi?acc=GSE13355, and https://www.ncbi.nlm.nih.gov/geo/query/acc.cgi?acc=GSE78097).

Received: 31 December 2023; Accepted: 1 October 2024

Published online: 11 October 2024

References

- 1. Cao, T. et al. Neutrophil extracellular traps promote keratinocyte inflammation via AIM2 inflammasome and AIM2-XIAP in psoriasis. Exp. Dermatol. 32, 368–378. https://doi.org/10.1111/exd.14711 (2023).
- 2. Hu, P. et al. The role of helper T cells in psoriasis. Front. Immunol. 12, 788940. https://doi.org/10.3389/fimmu.2021.788940 (2021).
- Kamata, M. & Tada, Y. Dendritic cells and macrophages in the pathogenesis of psoriasis. Front. Immunol. 13, 941071. https://doi. org/10.3389/fimmu.2022.941071 (2022).
- Li, Q. & Jiang, Y. Study on the correlation between morphology and distribution of common psoriasis lesions. Comput. Math. Methods Med. 2022, 6963630. https://doi.org/10.1155/2022/6963630 (2022).
- 5. Armstrong, A. W. & Read, C. Pathophysiology clinical presentation, and treatment of psoriasis: A review. *Jama* 323, 1945–1960. https://doi.org/10.1001/jama.2020.4006 (2020).
- Papp, K. A. et al. Treatment satisfaction, safety and effectiveness of adding methotrexate to adalimumab in patients with psoriasis
 responding suboptimally to adalimumab in a real-world setting. Br. J. Dermatol. 186, 726–728. https://doi.org/10.1111/bjd.20885
 (2022).
- Yan, M. et al. Neutrophil extracellular traps in tumor progression and immunotherapy. Front. Immunol. 14, 1135086. https://doi. org/10.3389/fimmu.2023.1135086 (2023).
- 8. Wigerblad, G. & Kaplan, M. J. Neutrophil extracellular traps in systemic autoimmune and autoinflammatory diseases. *Nat. Rev. Immunol.* 23, 274–288. https://doi.org/10.1038/s41577-022-00787-0 (2023).
- 9. O'Neil, L. J. et al. Neutrophil extracellular trap-associated carbamylation and histones trigger osteoclast formation in rheumatoid arthritis. *Ann. Rheum. Dis.* 82, 630–638. https://doi.org/10.1136/ard-2022-223568 (2023).
- Hidalgo, A. et al. Neutrophil extracellular traps: from physiology to pathology. Cardiovasc. Res. 118, 2737–2753. https://doi. org/10.1093/cvr/cvab329 (2022).
- Wilson, A. S. et al. Neutrophil extracellular traps and their histones promote Th17 cell differentiation directly via TLR2. Nat. Commun. 13, 528. https://doi.org/10.1038/s41467-022-28172-4 (2022).
- Zhou, G. et al. Exploring the association and causal effect between white blood cells and psoriasis using large-scale population data. Front. Immunol. 14, 1043380. https://doi.org/10.3389/fimmu.2023.1043380 (2023).
- Lambert, S. et al. Neutrophil extracellular traps induce human Th17 cells: Effect of psoriasis-associated TRAF3IP2 genotype. J. Investig. Dermatol. 139, 1245–1253. https://doi.org/10.1016/j.jid.2018.11.021 (2019).
- 14. Wu, J. et al. Identification of renal ischemia reperfusion injury subtypes and predictive strategies for delayed graft function and graft survival based on neutrophil extracellular trap-related genes. *Front. Immunol.* 13, 1047367. https://doi.org/10.3389/fimmu.2022.1047367 (2022).
- 15. Ritchie, M. E. et al. Limma powers differential expression analyses for RNA-sequencing and microarray studies. *Nucleic Acids Res.* 43, e47. https://doi.org/10.1093/nar/gkv007 (2015).
- Ito, K. & Murphy, D. Application of ggplot2 to pharmacometric graphics. CPT Pharmacometrics Syst. Pharmacol. 2, e79. https://doi.org/10.1038/psp.2013.56 (2013).
- Langfelder, P. & Horvath, S. WGCNA: an R package for weighted correlation network analysis. BMC Bioinform. 9, 559. https://doi. org/10.1186/1471-2105-9-559 (2008).
- Wu, T. et al. Clusterprofiler 4.0: A universal enrichment tool for interpreting omics data. *Innovation (Cambridge)*. 2, 100141. https://doi.org/10.1016/j.xinn.2021.100141 (2021).
- Friedman, J., Hastie, T. & Tibshirani, R. Regularization paths for generalized linear models via coordinate descent. J. Stat. Softw. 33, 1–22 (2010).
- 20. Robin, X. et al. pROC: an open-source package for R and S+ to analyze and compare ROC curves. *BMC Bioinform.* 12, 77. https://
- doi.org/10.1186/1471-2105-12-77 (2011).
 Newman, A. M. et al. Robust enumeration of cell subsets from tissue expression profiles. *Nat. Methods* 12, 453–457. https://doi.org/10.1038/nmeth.3337 (2015).
- Zhang, X. et al. m6A regulator-mediated RNA methylation modification patterns are involved in immune microenvironment regulation of periodontitis. J. Cell. Mol. Med. 25, 3634–3645. https://doi.org/10.1111/jcmm.16469 (2021).
- 23. Livak, K. J. & Schmittgen, T. D. Analysis of relative gene expression data using real-time quantitative PCR and the 2(-delta delta C(T)) method. *Methods* 25, 402–408. https://doi.org/10.1006/meth.2001.1262 (2001).
- Kanehisa, M. & Goto, S. KEGG: kyoto encyclopedia of genes and genomes. Nucleic Acids Res. 28(1), 27–30. https://doi.org/10.1093/ nar/28.1.27.PMID:10592173;PMCID:PMC102409 (2000).
- Kanehisa, M. Toward understanding the origin and evolution of cellular organisms. *Protein Sci.* 28(11), 1947–1951. https://doi. org/10.1002/pro.3715 (2019).
- Kanehisa, M., Furumichi, M., Sato, Y., Kawashima, M. & Ishiguro-Watanabe, M. KEGG for taxonomy-based analysis of pathways and genomes. *Nucleic Acids Res.* 51(D1), D587–D592. https://doi.org/10.1093/nar/gkac963.PMID:36300620;PMCID:PMC9825424 (2023).
- 27. Kaltenmeier, C. et al. Neutrophil extracellular traps promote T cell exhaustion in the tumor microenvironment. Front Immunol. 12, 785222. https://doi.org/10.3389/fimmu.2021.785222 (2021).
- 28. Zhang, Y. et al. AIM2 and Psoriasis. Front Immunol. 14, 1085448. https://doi.org/10.3389/fimmu.2023.1085448 (2023).
- 29. Wang, J. et al. Roles of AIM2 gene and AIM2 inflammasome in the pathogenesis and treatment of psoriasis. Front. Genet. 13, 929162. https://doi.org/10.3389/fgene.2022.929162 (2022).
- 30. Sobolev, V. V. et al. Effects of expression of transcriptional factor AP-1 FOSL1 gene on psoriatic process. *Bull. Exp. Biol. Med.* 150, 632–634. https://doi.org/10.1007/s10517-011-1208-0 (2011).
- 31. Sobolev, V. V. et al. The role of transcription factor PPAR-γ in the pathogenesis of psoriasis, skin cells, and immune cells. *Int. J. Mol. Sci.* https://doi.org/10.3390/ijms23179708 (2022).
- 32. Piaserico, S., Orlando, G. & Messina, F. Psoriasis and cardiometabolic diseases: Shared genetic and molecular pathways. *Int. J. Mol. Sci.* https://doi.org/10.3390/ijms23169063 (2022).
- 33. Purzycka-Bohdan, D. et al. Analysis of the potential genetic links between psoriasis and cardiovascular risk factors. *Int. J. Mol. Sci.* https://doi.org/10.3390/ijms22169063 (2021).
- 34. Tupikowska-Marzec, M. et al. The influence of FTO polymorphism rs9939609 on obesity some clinical features, and disturbance of carbohydrate metabolism in patients with psoriasis. *Biomed. Res. Int.* 2019, 7304345. https://doi.org/10.1155/2019/7304345 (2019).
- 35. Voiculescu, V. M. et al. Gene polymorphisms of TNF-238G/A, TNF-308G/A, IL10-1082G/A, TNFAIP3, and MC4R and comorbidity occurrence in a Romanian population with psoriasis. *J. Med. Life* 11, 69–74 (2018).
- 36. Ogretmen, Z. et al. Association of endothelial nitric oxide synthase Glu298Asp gene polymorphism in psoriasis cases with hypertension. *Ann. Saudi Med.* 34, 340–345. https://doi.org/10.5144/0256-4947.2014.340 (2014).
- 37. Casas, J. P. et al. Endothelial nitric oxide synthase gene polymorphisms and cardiovascular disease: a HuGE review. Am. J. Epidemiol. 164, 921–935. https://doi.org/10.1093/aje/kwj302 (2006).
- Cheng, H. et al. Identification of a missense variant in LNPEP that confers psoriasis risk. J. Investig. Dermatol. 134, 359–365. https://doi.org/10.1038/jid.2013.317 (2014).
- 39. Qu, Y. et al. Transcriptional regulation on effector T cells in the pathogenesis of psoriasis. Eur. J. Med. Res. 28, 182. https://doi.org/10.1186/s40001-023-01144-0 (2023).

- 40. Chen, H. L. et al. Galectin-7 downregulation in lesional keratinocytes contributes to enhanced IL-17A signaling and skin pathology in psoriasis. *J. Clin. Invest.* https://doi.org/10.1172/jci130740 (2021).
- 41. Köks, S. et al. Possible relations between the polymorphisms of the cytokines IL-19, IL-20 and IL-24 and plaque-type psoriasis. Genes Immun. 6(5), 407-415. https://doi.org/10.1038/sj.gene.6364216 (2005).
- 42. Kõks, S. et al. Combined haplotype analysis of the interleukin-19 and -20 genes: relationship to plaque-type psoriasis. *Genes Immun.* 5(8), 662–667. https://doi.org/10.1038/sj.gene.6364141 (2004).
- 43. Lé, A. M. & Torres, T. New topical therapies for psoriasis. Am. J. Clin. Dermatol. 23(1), 13–24. https://doi.org/10.1007/s40257-021-00649-w (2022).
- 44. Hu, P. et al. The role of helper T cells in psoriasis. Front. Immunol. 15(12), 788940. https://doi.org/10.3389/fimmu.2021.788940 (2021).
- 45. Hong, D. et al. Profiling serum cytokines and anticytokine antibodies in psoriasis patients. J. Immunol. Res. 8(2022), 2787954. https://doi.org/10.1155/2022/2787954. (2022).
- Mellor, L. F. et al. Keratinocyte-derived S100A9 modulates neutrophil infiltration and affects psoriasis-like skin and joint disease. Ann. Rheum. Dis. 81, 1400–1408. https://doi.org/10.1136/annrheumdis-2022-222229 (2022).
- 47. Defrêne, J. et al. Deletion of \$100a8 and \$100a9 enhances skin hyperplasia and promotes the Th17 response in imiquimod-induced psoriasis. *J. Immunol.* **206**, 505–514. https://doi.org/10.4049/jimmunol.2000087 (2021).
- 48. Lee, Y. et al. S100A8 and S100A9 are messengers in the crosstalk between epidermis and dermis modulating a psoriatic milieu in human skin. *Biochem. Biophys. Res. Commun.* 423, 647–653. https://doi.org/10.1016/j.bbrc.2012.05.162 (2012).
- 49. Chimenti, M. S. et al. S100A8/A9 in psoriatic plaques from patients with psoriatic arthritis. J. Int. Med. Res. 44, 33–37. https://doi.org/10.1177/0300060515598900 (2016).
- 50. Wang, S. et al. S100A8/A9 in Inflammation. Front. Immunol. 9, 1298. https://doi.org/10.3389/fimmu.2018.01298 (2018).
- 51. Christmann, C. et al. Interleukin 17 promotes expression of alarmins \$100A8 and \$100A9 during the inflammatory response of keratinocytes. Front. Immunol. 11, 599947. https://doi.org/10.3389/fimmu.2020.599947 (2020).
- 52. Edgeworth, J. et al. Identification of p8,14 as a highly abundant heterodimeric calcium binding protein complex of myeloid cells. *J. Biol. Chem.* **266**, 7706–7713 (1991).
- 53. Gudmundsdottir, A. B. et al. Exopolysaccharides from cyanobacterium aponinum induce a regulatory dendritic cell phenotype and inhibit SYK and CLEC7A expression in dendritic cells, T cells and keratinocytes. *Int. Immunopharmacol.* 69, 328–336. https://doi.org/10.1016/j.intimp.2019.01.044 (2019).
- 54. Wu, D. et al. Disruption of C/EBPβ-Clec7a axis exacerbates neuroinflammatory injury via NLRP3 inflammasome-mediated pyroptosis in experimental neuropathic pain. *J. Transl. Med.* **20**, 583. https://doi.org/10.1186/s12967-022-03779-9 (2022).
- 55. de Figueiredo, A. M. B. et al. Genome-wide association study reveals CLEC7A and PROM1 as potential regulators of paracoccidioides brasiliensis-induction of cytokine production in peripheral blood mononuclear cells. J. Fungi (Basel). https://doi.org/10.3390/jof9040428 (2023).
- 56. Al Madhoun, A. et al. Dectin-1 as a potential inflammatory biomarker for metabolic inflammation in adipose tissue of individuals with obesity. *Cells*. https://doi.org/10.3390/cells11182879 (2022).
- 57. Al-Nakhle, H. H. & Khateb, A. M. Comprehensive in silico characterization of the coding and non-coding SNPs in human dectin-1 gene with the potential of high-risk pathogenicity associated with fungal infections. *Diagnostics (Basel)*. https://doi.org/10.3390/diagnostics13101785 (2023).
- 58. Ma, F. et al. Single cell and spatial sequencing define processes by which keratinocytes and fibroblasts amplify inflammatory responses in psoriasis. *Nat. Commun.* 14, 3455. https://doi.org/10.1038/s41467-023-39020-4 (2023).
- 59. Zou, A., Chen, Y., Liu, T., Yang, T. & Zhou, B. Identification and verification of three autophagy-related genes as potential biomarkers for the diagnosis of psoriasis. *Sci. Rep.* 13(1), 22918. https://doi.org/10.1038/s41598-023-49764-0 (2023).
- Liang, N. & Zhang, K. The link between autophagy and psoriasis. Acta Histochem. 126(4), 152166. https://doi.org/10.1016/j.acthis.2024.152166 (2024).
- 61. Douroudis, K. et al. Polymorphisms in the ATG16L1 gene are associated with psoriasis vulgaris. *Acta Derm. Venereol.* **92**(1), 85–87. https://doi.org/10.2340/00015555-1183 (2012).

Acknowledgements

The authors extend special thanks to all research students and researchers involved in this study.

Author contributions

Yike Zhao and Ling Wang wrote the main manuscript text. Xiaoguang Zhang and Lihua Zhang designed the work. Feng Wei and Suyue Li analyzed the data. Yanling Li revised the manuscript critically for important intellectual content. All authors reviewed the manuscript.

Funding

This research was funded by Hebei Province Department of Bureau of Science and Technology of China (No.202050801010015, No.202130806010002) and Health Commission of Hebei Province (No.20242044).

Declarations

Competing interests

The authors declare no competing interests.

Ethics approval and consent to participate

All procedures were approved by the Ethics Committee of the second hospital of Hebei Medical University (2023-R331).

Additional information

Supplementary Information The online version contains supplementary material available at https://doi. org/10.1038/s41598-024-75069-x.

Correspondence and requests for materials should be addressed to Y.L.

Reprints and permissions information is available at www.nature.com/reprints.

Publisher's note Springer Nature remains neutral with regard to jurisdictional claims in published maps and institutional affiliations.

Open Access This article is licensed under a Creative Commons Attribution-NonCommercial-NoDerivatives 4.0 International License, which permits any non-commercial use, sharing, distribution and reproduction in any medium or format, as long as you give appropriate credit to the original author(s) and the source, provide a link to the Creative Commons licence, and indicate if you modified the licensed material. You do not have permission under this licence to share adapted material derived from this article or parts of it. The images or other third party material in this article are included in the article's Creative Commons licence, unless indicated otherwise in a credit line to the material. If material is not included in the article's Creative Commons licence and your intended use is not permitted by statutory regulation or exceeds the permitted use, you will need to obtain permission directly from the copyright holder. To view a copy of this licence, visit http://creativecommons.org/licenses/by-nc-nd/4.0/.

© The Author(s) 2024